High-level Sizing Method for Hybrid Electric Distributed Propulsion Aircraft

Baptiste Legrand[1,3,†], *Nicolas Curlier*[3], *Arnaud Gaillard*[2] *and David Bouquain*[1]
[1]*Université de Franche-Comté, UTBM, CNRS, Institut FEMTO-ST, Belfort, France*
[2]*UTBM, CNRS, Institut FEMTO-ST, Belfort, France*
[3]*Avions Mauboussin, Belfort, France*
[†]baptiste.legrand@femto-st.fr

Abstract

New concepts of aircraft and new energy carriers in aeronautics challenge aircraft design processes. Essential early design stages such as conceptual and preliminary design are significantly affected. During this stage, sizing methods commonly rely on historical datasets and laws. However substantial differences between conventional and new aircraft beg to question the representativeness of these assumptions. The following study strives to answer the issue of aircraft preliminary sizing through a model-based design approach. A full range of design and interpretations on their feasibility are showcased.

1. Introduction

Diversification of aircraft constraints such as low noise or low carbon footprint aircraft arise from regulations and new consumer needs. Historic and emerging aircraft manufacturer are developing new aircraft concepts to answer these needs. Under guidance of these manufacturers, key enabling technologies such as electrification or hydrogen propulsion systems grow at a rapid pace. However upcoming integration of these technologies in an aircraft puts into perspective the way aircraft are sized.

Aircraft architecture, system mass and integration, power management of new propulsion systems... are fundamental differentiators between conventional and new aircraft concepts. With hybridization or power distribution [1, 2] the purview of the propulsion system is redefined. Propulsion system which is conventionally used to propel the aircraft, could enhance lift or drag, propose additional steering features or even provide truly high redundancy with these new concepts. However, the issue of the validity and representativeness of sizing methods [3–6] and their associated laws still remains.

Several really promising tools such as OpenConcept [7], SUAVE [8] or FastOAD [9] are trying to answer the sizing issues of novel aircraft design. However most of these tools are still under development thus providing a limited number of models to represent an aircraft. The method developed hereafter takes into consideration additional physic fields such as aeropropulsive interaction and power management. The method is built upon model-based design principles giving the user freedom in the design of its aircraft. The tool developed after this method allows the user to design the aircraft throughout the mission or study trade-off with specific design variables. This article is divided in two major sections. The first section highlights the aircraft design methodology while the second section provides a case study on design exploration of a 12-seater aircraft.

2. Design process

2.1 Method

This method is applied to complex aircraft and propulsion architectures. Therefore, models and assumptions need to be easy to understand and identify. Model-based design principles answer such constraints. Each component or physic interaction is represented by one or multiple models with similar inputs, thus enabling upgradability. Different design level can be compared for aircraft preliminary sizing. Figure 1 details the different components and physic fields integrated in the methodology. Intermediate steps and models are described in the Models section 2.3. The method is split in three major sections : aircraft design, powertrain design and analysis. Aircraft design and powertrain design are built around two principles lift-drag assessment and power management.

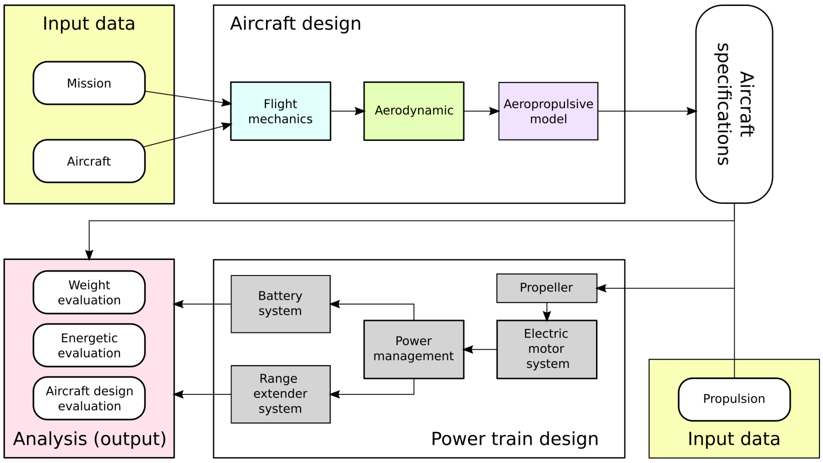

Figure 1: General preliminary sizing approach

The aircraft design revolves around the assessment of lift and drag coefficient (C_L and C_D). This design phase starts with the definition of flight requirements through a model of the flight mechanics and the aerodynamic of the wing. At this step, a first assessment of C_L and C_D is done. This assessment results in the choosing of the aircraft aeropropulsive model. More detail about this model is given in section 2.3.2.

Aircraft specifications are then used as entry data for the powertrain design. A propeller model enables the conversion of traction requirement to the shaft power requirement. Energy transfer concept are used to dispatch power requirements from one component to the other. During the sizing process power management assigns each source with a share of the energy required to propel the aircraft. More detail about this step is given in section 2.3.3.

2.2 Inputs, design variables and outputs

The objective of preliminary design is to study trade-off between aircraft and propulsion architecture through the evolution of some characteristics. Therefore inputs, design variables and outputs should be carefully considered on a global scale. Low level design variables require fine models and finer models require more input data. This leads to a great number of inputs which might be undefinable at this stage of the design process. Another consequence is the increase in the complexity and computing time of the global model.

The inputs of the design process are divided in three categories : mission profile, aircraft characteristics and propulsion characteristics. The mission profile is composed of plane speed, altitude and duration for each phase. The aircraft and propulsion characteristics are defined by the designer. Lists of the major aircraft and propulsion characteristics are given throughout section 3.1.

The design variables are indexed in a short list of inputs of interest to the designer. This list largely depends on the problematic at hand. A feasibility study aiming to demonstrate the impact of a component technology on the aircraft will most likely require a small amount of propulsion inputs as design variable. On the other hand a complete aircraft preliminary sizing study might require mission, aircraft and propulsion inputs as design variables. As the subject of this research paper is the study of the influence of the aircraft design on the powertrain and aircraft feasibility, the most part of the design variables are aircraft characteristics.

The outputs of the design process are the traction requirement for the aircraft specifications, the aircraft mass budget and the power profile for a given configuration. The mass budget as well as the required traction plead for the feasibility of the design. The power profile informs the designer on how the power management rules translates into the components sizing requirements.

2.3 Models

2.3.1 Aircraft performance, flight mechanics and aerodynamics

Aircraft performance regroups a set of models allowing the definition the aircraft requirements for a contingent mission profile and aircraft specifications. It is based on the flight mechanics and aerodynamics analysis of the aircraft.

The flight mechanics model returns the lift and drag assessment then translated in required C_L and C_D. The most commonly used model is a derivative of the Fundamental Principle of Dynamics. The aerodynamic model computes the C_L and C_{Di} of the conventional lift enhancement devices such as the wing or the flaps. Frequently used model are the Lifting Line Theory or the Vortex Lattice Method. The choosing of the model is usually driven by the computional efficiency as well as representativeness and accuracy. In the case of the developed method analytical models such as Lifting Line Theory are favoured for their low computing cost.

The lift and drag coefficient resulting from the aerodynamic and flight mechanics model are integrated in the assessment displayed with the equations 1a and 1b.

$$C_L = \sum C_{L_n} \tag{1a}$$

$$C_D = C_{D0} + \sum C_{Di_n} \tag{1b}$$

Where n is a defined contributor such as the wing, the flaps, the distributed propulsion and others.

2.3.2 Aeropropulsive

Aeropropulsive models tie the propulsion system and the aircraft performances together. These models enable the definition and study of novel propulsion architectures. Concepts such as distributed propulsion [10], wing-tip mounted propeller [11], counter-rotative propeller, boundary layered ingestion turbine [12] and others are vastly studied as a solution for different constraints. In the following research work the constraint studied falls in the performance enhancement category, especially on lift enhancement using distributed propulsion.

In the case of lift enhancement, the choice between distributed and conventional propulsion model is ruled by the maximal wing lift and flight segment required lift. Conventional propulsion model is used when wing C_L reaches required C_L before stall. Otherwise the aeropropulsive model provides the remaining C_L to reach the flight segment requirement. A similar logic is applicable for drag enhancement features.

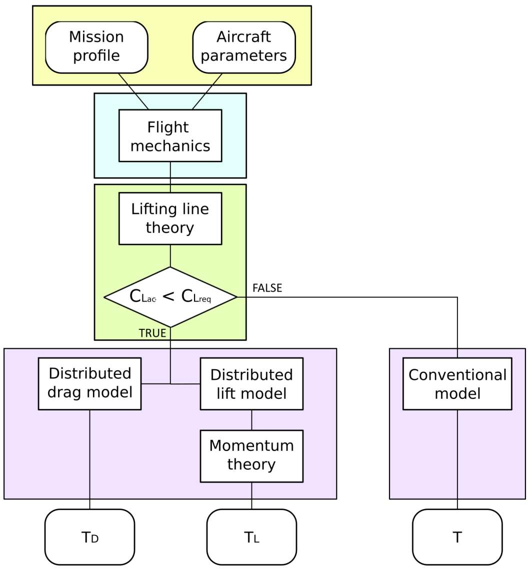

Figure 2: Aeropropulsive algorithmic model for distributed propulsion architecture

Figure 2 shows the logic resulting in the sizing of the propulsion requirements. For distributed propulsion concepts, the relationship between airfoil C_L and airflow speed [13] is used. The excess speed necessary to reach the lift coefficient required is provided by the distributed propeller. Coupled with momentum theory, the speed is translated to a required traction named lift traction (T_L). T_L is then compared to traction requirement resulting from drag, which is named drag traction (T_D). After computing the required tractions, the aeropropulsive model is interfaced with a propeller model to define the required shaft power.

2.3.3 Powertrain

Powertrain sizing is rooted in the use of multi-physics energy transfer assumptions and the assessment of the power management. Multi-physics energy transfer assumption allows the build up of a power requirement in a component as defined in equation 2.

$$P_{in} = P_{loss} + P_{out} \tag{2}$$

P_{loss} formulation changes with the model used. For example with fixed efficiency models P_{loss} value is directly proportional to P_{in} or P_{out} regardless of the value of their derivatives. Power requirements are then transmitted from one component to another to size the system. Power derivates can be transmitted along thus enabling the use of more complex component models.

When hybrid propulsion systems are studied the energy distribution between sources is not trivial. Therefore an assessment of the power management is necessary. A number of power management strategies can be found in literature [14] such as rule-based, fuzzy logic or dynamic programming. Different criteria such as efficiency, fuel consumption or speed can be optimized with the power management.

Power management drives the definition of two indicators [15, 16], hybridization ratio and power ratio. These indicators, describe the load on the components of the powertrain at a defined flight point. The hybridization ratio compares the power drawn from each source to the power requirement at a given flight point. The power ratio compares the power drawn from a source at a given flight point to the maximal power this source can provide. This philosophy is applicable to different types of architectures and power management.

3. Case study

3.1 Hypothesis and entry data

3.1.1 Mission profile

The objective is to study a short take-off distance aircraft with a reasonable cruise speed and range. The conventional mission profile is built in 5 phases. These phases are take-off, climb, cruise, descent and landing. Each phase has an associated plane speed, altitude start, altitude end and duration. Table 1 provides the range of flight performance for the typical mission. A number of flight segments are deduced from this table for each phase.

Table 1: Mission profile

Phase	Speed (m/s)	Altitude (m)	Duration (s)
TO	[0 - 28]	[0 - 15]	15
Climb	[35 - 70]	[15 - 950]	560
Cruise	[80 - 85]	[950 - 950]	18000
Descent	[70 - 50]	[950 - 15]	480
LA	[30 - 0]	[15 - 0]	15

NOTE : for a phase, [start value - end value]

Regarding take-off and landing, the following assumptions table 2 are added.

Table 2: Take-off and landing assumptions

Characteristic	Take-off	Landing	Unit
Total distance	300	300	m
Obstacle height	15	15	m
Friction/breaking coefficient	0.05	0.5	-
Load factor	1.193	1.253	

3.1.2 Aircraft configuration

The aircraft configuration is based on the hypothesis set listed below.

- Tube and wing configuration.
- No tapper ratio or twisted sections for the wing.
- Fuselage diameter is substracted from wing span for lift estimation.

Table 3 displays the aircraft configuration typical values used for the sensitivity study.

Table 3: Aircraft characteristics

Characteristic	**Value**	**Unit**
MTOW	3000	kg
Wing area	25	m^2
Fuselage diameter	1.5	m
Aspect ratio	10	-
Wing profile	NACA 2408	-
Aircraft parasitic drag	0.02	-
Flaps additional CL	0.7	-

3.1.3 Distributed propulsion

The distributed propulsion model [13] represents a leading edge propulsion system. The following set of hypothesis is assumed.

- Propellers cover and blow the whole wing area.
- Thin airfoil theory hypothesis.
- Blade momentum theory hypothesis.
- No stall sections on the wing after the propeller.
- Model is valid for propeller integration angles from -10 to 10 degrees.
- Parasitic drag associated with distributed propulsion integration is not considered.

The set of typical values for the distributed propulsion is displayed in table 4.

Table 4: Distributed propulsion characteristics

Characteristic	**Typical value**	**Unit**
Number of propeller	18	-
Propeller integration angle	-5	°
Fuselage diameter	1.5	m
Propeller model	DUC 5-blades	-
Blown surface	Wing area	-

3.1.4 Powertrain hypothesis

The powertrain architecture evaluated hereafter is based on hybrid series architecture, shown in figure 3. This configuration has been chosen regarding two factors, enabling of distributed propulsion and enabling of hydrogen propulsion system with thermal machines or fuel cells. The powertrain is built around two main drivetrains. The distributed drivetrain is switch on during high lift phases while the conventional drivetrain is switch on during normal flight phases and high lift phases if needed. The distributed drivetrain is composed of *2n* similar drivetrains *a* while the conventional drivetrain is composed of 1 drivetrain *b*.

Energy can flow in multiple directions, from sources to propeller, from propeller to battery system, from range extender system to battery system. However, efficiency might differ in normal and reverse mode for some systems.

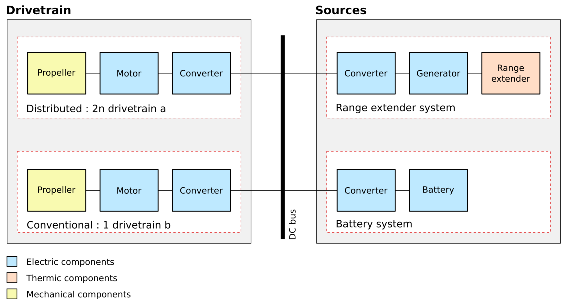

Figure 3: Hybrid series powertrain architecture

The first estimate of the propulsion components characteristics given in table 5 is based on a state of the art. Accurately estimating these characteristics is mandatory as strong evolution in the sizing of the propulsion system could arise from different assumptions. For example the high-speed/low-torque electric motors are able to multiply by 5-10 times the power density of a low-speed/high-torque motor [17]. However, high speed electric motor requires a gearbox to reduce the rotational speed to acceptable limits for the propeller.

Table 5: Characteristics of propulsion system components

Component	**Efficiency**	**Power density (W/kg)**	**Energy density (Wh/kg)**	**Reference component**
Electric motor/generator	0.95	2 500	-	Emsiso 348
Power electronic interfaces	0.95	10 000	-	emDrive H300
Battery	-	1 600	200	Sony VTC6
Turbine	0.25	3 000	-	PT6A

The range extender characteristics are based on a PT6A [18] turbine as this type of turbine is well documented. The preliminary sizing of batteries is usually a scale-up of the cell characteristics. However, in this case an integration factor estimating the total battery mass based on the mass of chemistry is added. A first order estimation of that factor is 1.6.
The power management for the case study aircraft relies on the following rules :

- Fixed-efficiency assumption is made on the basis that the different system will operate close to their typical operating point.
- Range-extender provides 100 % of the power for a cruise flight segment. Hybridization offsets the lack of power when needed.
- Powertrain is in hybrid mode as long as required power exceed range-extender maximal available power.
- Distributed propulsion is sized on take-off constraints.
- Power is based on the largest traction requirement between T_L and T_D regarding the following rules.
  - If $\mathrm{T_L} > \mathrm{T_D}$ aircraft traction is $\mathrm{T_L}$. Distributed propulsion provides this traction alone.
  - If $\mathrm{T_L} \leq \mathrm{T_D}$ aircraft traction is $\mathrm{T_D}$. Distributed propulsion provides $\mathrm{T_L}$ while conventional propulsion provides $\mathrm{T_D} - \mathrm{T_L}$

3.2 Design variables

The choice of design variables depends on what the designer wants to prove. The question investigated here is the influence of major aircraft design characteristics on the aircraft and powertrain design. Henceforth, the major design variables are displayed in table 6.
During a variable study the typical value is used for every other variable. These design variables are expected to be key factor in the sizing of the aircraft and its propulsion system. A sensitivity study is conducted on each of the variables to better understand their influence on the design.

Table 6: Design variables of interest

Design variable	Typical value	Minimal value	Maximal value
Number of distributed drivetrains	18	6	34
Maximal Take-Off Weight	3000 kg	2500 kg	4000 kg
Wing area	25 m^2	20 m^2	35 m^2
Aspect ratio	10	4	12
Distributed propeller integration angle	-5°	-7.5°	0°
Fuselage diameter	1.5 m	1.5 m	2 m

3.3 Preliminary results and interpretations

3.3.1 Influence of distributed propeller count on the design

In aeronautics, feasibility of a design is closely related to the estimated aircraft mass. Most of the design processes iterate on the maximal take-off weight through a first guess. This study proposes a similar approach. The results presented in this subsection will serve as an example to provide clues on the interpretation of other results, while evaluating distributed propeller count as a design variable.

As stated section 2.2 feasibility is verified through the analysis of two results : the traction equilibrium and mass assessment. During high lift segment, where distributed propulsion is used to provide lift, the aircraft traction is a combination of the drag and lift required traction. Lift traction and drag traction result from different physic phenomenon as previously explained. Therefore over-traction in high lift phases is common [13]. In the figure 4 the over-traction region is coloured. The traction equilibrium requires a distributed propulsion configuration of around 18 motors. More motors means that traction requirement is split between distributed and conventional propulsion systems. The conclusion from these results means that more motors reduces the burden on the distributed propulsion system.

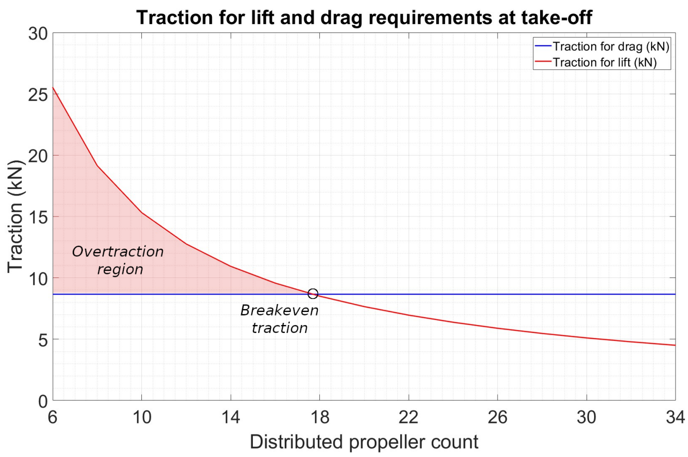

Figure 4: Traction requirements as a function of distributed propeller count

However feasibility is also evaluated through mass system. Figure 5 shows the mass evolution through the distributed propeller range. An interesting behaviour on the mass evolution of the systems is displayed. After crossing the break-even traction point, the mass of the whole system converges around 700 kg. This low evolution rate is a result of T_L and T_D assumption. After the break-even point, traction requirement is constant resulting in a quasi-constant aircraft power requirement.

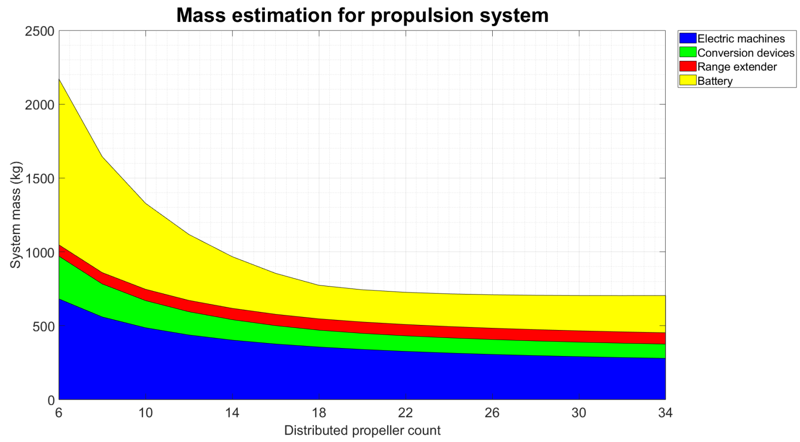

Figure 5: Propulsion system mass budget as a function of distributed propeller count

The quasi-constant power requirement hypothesis is displayed in table 7. Slight variations in the shaft power are induced by the modification of the propeller operating point between the configurations. The induced variation on the power is of the order of 5 % in this energetic study. As the components of the powertrain have a constant efficiency this variation will remain similar throughout the studied configurations.

Table 7: Power requirements for distributed and conventional drivetrains

	18 distributed motors		**34 distributed motors**	
Component	Distributed	Conventional	Distributed	Conventional
Propeller shaft	386.9 kW	5.3 kW	204.8 kW	208.8 kW
Machine electric input	407.2 kW	5.6 kW	215.6 kW	219.7 kW

Despite low evolution rate after 18 propellers when picturing the system as a whole, the subsystems and components mass display a clear evolution. The figure 6 show the mass share of each component associated with their subsystems.

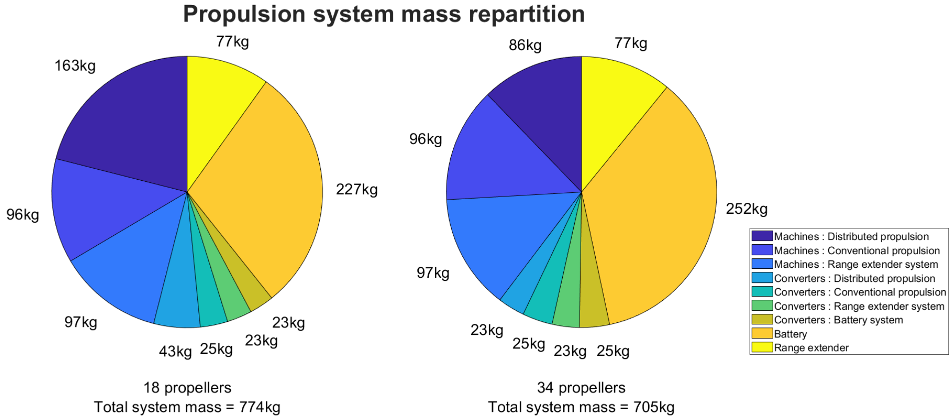

Figure 6: Components mass distribution for 18 and 34 distributed drivetrains

The range-extender system as well as the conventional drivetrain do not see any evolution. The first case is explained by the power-management assumptions. Hypothesis states that the range extender is sized to provide the power cruise demand. The second case is explained by the power requirement of this subsystem. Power requirement is assumed maximal during the second climb segment for both configurations.

On the other hand, distributed drivetrain and battery system display some evolution. The distributed drivetrain shows a downsizing with the increase of motor count. This subsystem power demand is usually maximal during take-off. The battery mass shows a slight increase resulting from the divergence of power requirements after the propeller.

3.3.2 Influence of other variables

In this section the results of the five other design variables are displayed. The study of these variables follows the strategy in the previous section 3.3.1. Most of the variables studied display monotonic evolution when comparing mass share of the components. However, in the case of wing area (figure 7) and wing aspect ratio (figure 8) a different mass evolution is displayed. A minimum propulsion system mass different from the one defined with the typical configuration is reachable. This behaviour is displayed in figures 7 and 8.

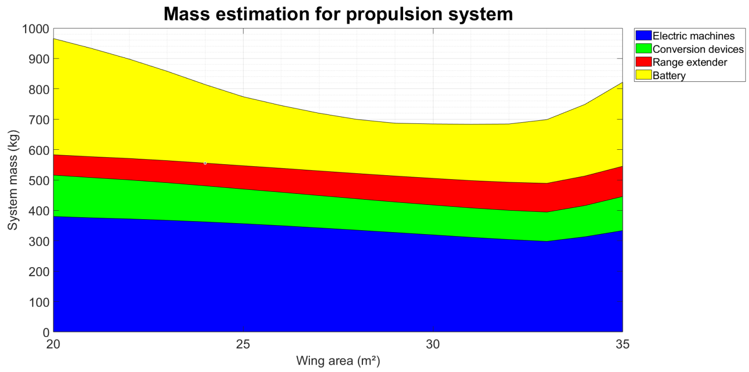

Figure 7: Propulsion mass system regarding wing area

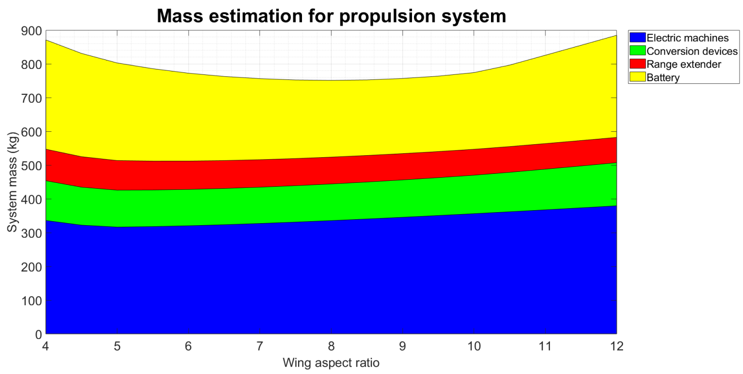

Figure 8: Propulsion mass system regarding wing aspect ratio

In the case of maximal take-off weight as a variable, displayed in figure 9, the system mass evolution alone doesn't provide enough information to conclude on the design feasibility. An additional red curve entitled "Payload and plane available mass" shows the remaining mass for the aircraft structure, payload and fuel. When maximal take-off weight is studied as a design variable, the optimum sizing point is not the lowest system mass but rather the highest payload and plane mass availability. This sizing point is in-between 3000 and 3100 kg.

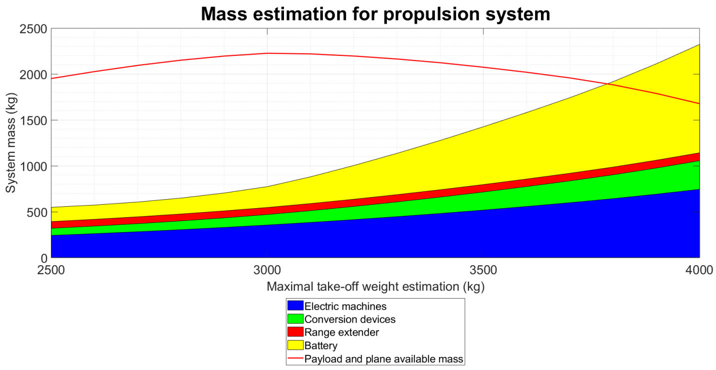

Figure 9: Propulsion mass system regarding maximal take-off weight guess

Propeller integration angle, in figure 10, displays non negligible evolutions throughout its studied range. As a design variable, it could help the designer to relieve mass constraints on the propulsion system. However, with the assumption on parasitic drag, the results shown are optimistic, especially for higher angles. Variations of parasitic drag especially at higher speed could alter the energy sizing point thus modifying the range extender and battery mass.

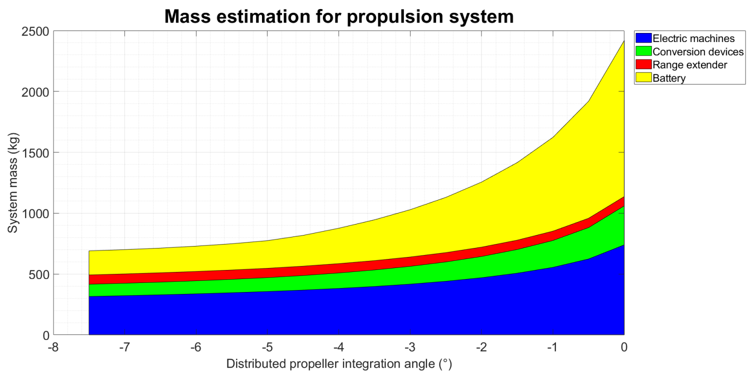

Figure 10: Propulsion mass system regarding distributed propeller integration angle

Finally, the fuselage diameter would be a noticeable variable to compare aircraft configurations such as tube and wing and blended wing body. The results shown figure 11 display mass improvement with higher fuselage diameter. However the assumptions made on aerodynamic drag limit the interpretations of these results.

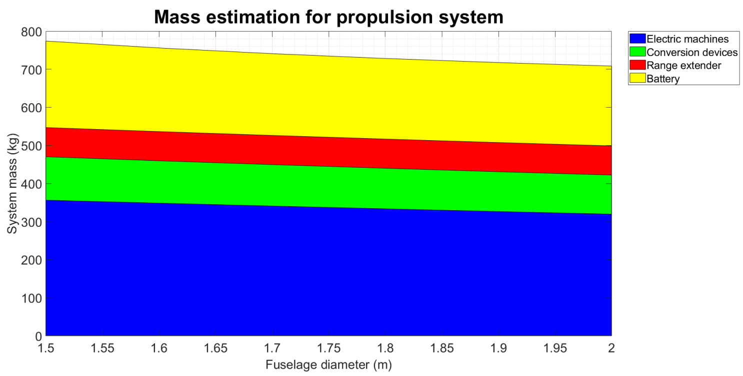

Figure 11: Propulsion mass system regarding fuselage diameter

As a conclusion of this study, the table 8 displays the minimal mass budget for each design variables and for which value it is reached. As stated during the assessment of the results, reaching the minimal system mass does not imply having the optimal sizing point, especially for maximal take-off weight.

Table 8: Synthesis of break-even tractions and minimal system mass values

Design variable	Break-even traction	Minimal mass	Minimum system mass (kg)
Distributed propeller count	17.8	32	704 kg
MTOW	3020 kg	2500 kg	549 kg
Wing area	24.5 m^2	31 m^2	683 kg
Aspect ratio	10.2	8	751 kg
Propeller integration angle	-4.8°	-7.5°	690 kg
Fuselage diameter	1.5 m	2 m	708 kg

Table 9 is given to compare the distributed drivetrain mass budget with similar conventional aircraft engines.

Table 9: State of art of comparable 11 to 14 seater aircraft

Aircraft	Aircraft type	Passengers	Engine	Total engine dry mass
DHC-3-Otter	Propeller	11	1 x PW R-1340	365kg
Tecnam P2012	Propeller	11	2 x TEO-540-C1A	502kg
Caravan	Propeller	14	1 x PT6A-114A	163kg
Kingair 360	Propeller	11	2 X PT6A-60A	442kg

As shown in the table 8, the lowest system mass is different from the typical values assumed for every variable. This means that one or multiple optimal configurations different from the typical values are reachable. A multi-variable analysis could provide more insight on how the system mass behaves.

3.3.3 Coupled variable study

Sensitivity study remains fairly limited when one variable is considered. Based on the previous results it appears that 3 variables are of interest : count of distributed propeller, wing area and wing aspect ratio. The range of these three variables remains the same. This set of variable gives a first order of the aeropropulsive configuration needed to propeller the aircraft in every condition. The figure 12 gives some insights on the system mass evolution trough the design space considered. Only 3 wing area values are displayed to improve the readability of the graphic.

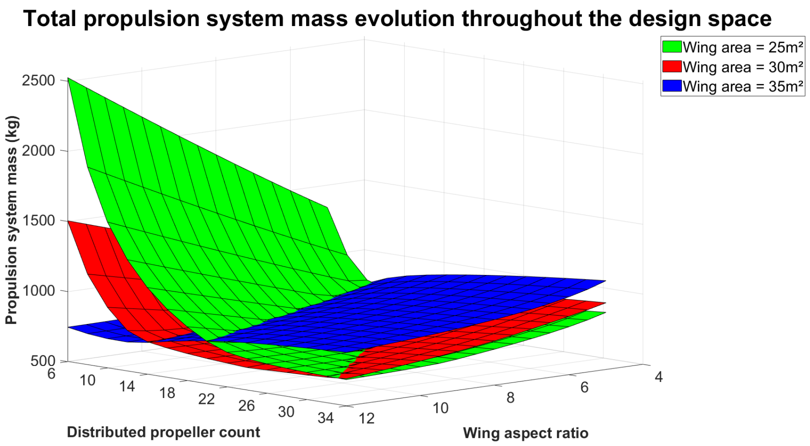

Figure 12: Mass evolution throughout the design space

The lowest mass estimation made for these three variables is a configuration of 24 propellers, an aspect ratio of 12 and a wing area of 30 m^2. The total system mass reaches 662kg improving the previously lowest mass configuration by 3 %. The figure 13 is a pie chart that displays the system mass repartition for this configuration.

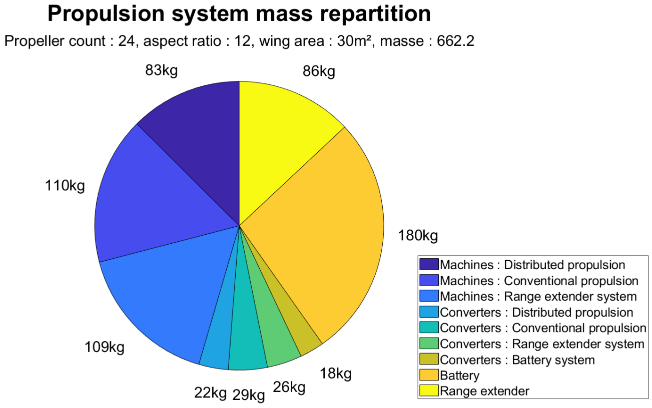

Figure 13: Components mass distribution for lowest mass

This mass assessment is the lowest propulsion system mass reachable. However if every system is taken alone, even lower system mass are reachable. The table 10 references the lowest mass for each system and the aircraft configuration where it is achieved.

Table 10: Minimal achievable system mass

System	Configuration	System mass (kg)	Propulsion system mass (kg)
Distributed drivetrain	[34 - 10.5 - 35]	20.4	907.4
Conventional drivetrain	[6 - 12 - 20]	102.6	3288.5
Battery	[20 - 12 - 28]	186.3	689.3
Range extender	[6 - 12 - 20]	165.9	3288.5

NOTE : variable order in configuration is [Propeller count - Aspect ratio - Wing area]

These results confirm the conclusion in section 3.3.2. A minimum mass far from the typical value first presented is reachable. In this study, the minimum reached remains local as the upper limit of the wing aspect ratio is reach. Issues might appear with the design and manufacturability of the wing with higher aspect ratio.

4. Discussions and conclusion

This paper proposes a complete methodology to run coupled sizing analysis on novel aircraft architectures. The reached conclusion questions the use of this type of aircraft architecture. Regarding the mass assessment, distributed propulsion system results in significant mass increase compared to conventional propulsion systems. This excess mass benefits limited time phase at the expense of payload or range. Distributed propulsion power management should lead to optimum energy consumption while maintaining acceptable mass budgets. These new approaches require to take into account variable efficiency to accurately size long flight phases. Moreover, the influence of the following assumptions needs to be taken in consideration.

1. Fixed efficiency carries a significant weight for the sizing of the powertrain and the aircraft. Most of the components used in current powertrain are granted with an optimal operating as a function of the load.

2. Fixed density for some components does not represent the whole range of available components. Electric motors that are categorized in torque or rotational speed have different density. High torque tends toward low power densities while high speed tends toward high power densities.

3. Aircraft mass assumptions such as fuselage or wing are lacking for a complete mass budget analysis. A first order analysis could be based on classic literature. However strong aeropropulsive coupling and new types of mass distributions might require a rework of these laws.

4. The limited amount of drag hypothesis decreases the accuracy of the sizing for some variables such as fuselage diameter or distributed propeller integration angle.

5. Multi-variable computing is time extensive. With large sets of variables and small steps, optimization processes such as Particle Swarm Optimization and Genetic Algorithm could cut down computing time.

The next step is to address part of these issues through modification of the powertrain components models. A more accurate study is achievable through the introduction of real components data and efficiency maps in the models.

5. Acknowledgement

This research work is supported by EIPHI (ANR-17-EURE-0002 contract), ANRT and Avions Mauboussin.

References

[1] D. Finger, F., C. Braun, and C. Bil. An initial sizing methodology for hybrid-electric light aircraft. 2018.

[2] R. de Vries, M. Brown, and R. Vos. A preliminary sizing method for hybrid-electric aircraft including aero-propulsive interaction effects. In *2018 Aviation Technology, Integration, and Operations Conference*, 2018.

[3] S. Gudmundsson. *General Aviation Aircraft Design : Applied Methods and Procedures*. Elsevier, 2014.

[4] P. D. Raymer. *Aircraft Design : A Conceptual Approach*. AIAA Education Series, second edition edition, 1992.

[5] J. Roskam. *Airplane Design : Part I - II*. DARcorporation, 2004-2005.

[6] J.D. Anderson. *Aircraft Performance and Design*. McGraw Hill, 1999.

[7] B. J. Brelje and J. R. R. A. Martins. Development of a conceptual design model for aircraft electric propulsion with efficient gradients. In *Proceedings of the AIAA/IEEE Electric Aircraft Technologies Symposium*, 2018.

[8] T. Lukaczyk, A. D. Vendorff, and E. Botero. Suave : An open-source environment for multi-fidelity conceptual vehicle design. 2015.

[9] Christophe David, Scott Delbecq, Sebastien Defoort, Peter Schmollgruber, Emmanuel Benard, and Valerie Pommier-Budinger. From FAST to FAST-OAD: An open source framework for rapid overall aircraft design. *IOP Conference Series: Materials Science and Engineering*, 1024(1):012062, jan 2021.

[10] Jean Hermetz, Michael Ridel, and Carsten Doll. Distributed electric propulsion for small business aircraft a concept-plane for key-technologies investigations. In *ICAS 2016*, DAEJEON, South Korea, September 2016.

[11] Mauro Minervino, Giovanni Andreutti, Lorenzo Russo, and Renato Tognaccini. Drag reduction by wingtip-mounted propellers in distributed propulsion configurations. *Fluids*, 7(7), 2022.

[12] David K. Hall, Arthur C. Huang, Alejandra Uranga, Edward M. Greitzer, Mark Drela, and Sho Sato. Boundary layer ingestion propulsion benefit for transport aircraft. *Journal of Propulsion and Power*, 33(5):1118–1129, 2017.

[13] Michael Patterson, Joseph Derlaga, and Nicholas Borer. High-lift propeller system configuration selection for nasa's sceptor distributed electric propulsion flight demonstrator. Jun 2016.

[14] A. Chauvin. *Contribution à l'optimisation globale pour le dimensionnement et la gestion d'énergie de véhicules hybrides électriques basée sur une approche combinatoire*. Theses, INSA de Lyon, November 2015.

[15] A. Isikveren, S. Kaiser, C. Pornet, and P. Vratny. Pre-design strategies and sizing techniques for dual-energy aircraft. *Aircraft engineering and aerospace technology*, 86:525–542, 10 2014.

[16] M. Marwa, B. Martos, M. S. Martin, and R. Anderson. Analytical forms of the range performance of hybrid and electric turboprop aircraft, for design optimization studies. In *55th AIAA Aerospace Sciences Meeting*, 2017.

[17] Ayman El-Refaie and Mohamed Osama. High specific power electrical machines: A system perspective. *CES Transactions on Electrical Machines and Systems*, 3(1):88–93, March 2019.

[18] Type Certificate Data Sheet PT6A-67 series. Technical report, EASA, 2022.